



Research on construction and application of macroeconomic forecasting model based on time series clustering analysis

Dezhi Yang^{1,*}

¹ Eastern Liaoning University, College of Science, Dandong 118003, Liaoning, China

SUMMARY: *In order to improve the accuracy of macroeconomic forecasting under complex time fluctuations, this paper proposes a multivariate macroeconomic data clustering enhanced forecasting framework combining time series clustering, sequence learning and residual correction. The framework first divides the 18 core indicators in the quarterly data of 12 years into homogeneous dynamic groups, then maps the clustering pattern into a time series prediction structure, and finally introduces a residual correction module to improve the output stability. Experiments were conducted on 1152 samples constructed according to indicators such as GDP growth, CPI, unemployment rate, industrial production, export, interest rate and investment. Compared with ARIMA, SVR and LSTM alone, the mean square error of the proposed method is reduced to 1.67%, the mean absolute error is reduced to 2.14%, and the root mean square error is reduced to 2.36%, and the average prediction accuracy is 93.41%. The results show that the model has strong robustness and good trend tracking ability, and has practical value for computer macroeconomic monitoring and forecasting across economic cycles and multi-index interaction scenarios.*

KEYWORDS: *Time series clustering; Macroeconomic forecasting; Temporal modeling; Error correction*

1 Introduction

In the process of macroeconomic operation, indicators such as growth, price, employment, investment, consumption and foreign trade do not change in isolation, but evolve together with different frequencies and different rhythms, forming a dynamic system with significant time series dependence. In the face of high-dimensional macro statistical data, the traditional analysis method relying on linear assumption and single stationary condition has been difficult to fully describe the complex relationship between index linkage, stage switching and volatility transmission. Time series modeling techniques, based on computer methods, are pushing macroeconomic forecasting from empirical judgment to data-driven calculation. Goulet Coulombe et al. studied the applicability of machine learning in macroeconomic forecasting and pointed out that nonlinear learning mechanism can form more resilient forecasting results in high-dimensional information environment [1]. Longo et al. proposed a neural network ensemble method for GDP forecasting, indicating that multi-model collaboration can enhance the fitting ability and output stability of economic series [2]. Lin studied the prediction method of US GDP based on empirical mode decomposition and deep learning, and proved that decomposition processing could help to improve the representation

*18704155188@163.com

<https://doi.org/10.65102/is20261025>

quality of complex sequences [3]. Wang et al. proposed a mixing error correction prediction method based on principal components, which provided a feasible path for the joint calculation of cross-frequency economic indicators [4]. Zhang et al. studied the performance of machine learning algorithms in the real-time prediction of China's GDP in a data-intensive environment, showing the supporting effect of large-scale index input on the efficiency of prediction update [5].

Existing research provides a computational basis for macroeconomic forecasting. However, from the perspective of model organization, the results emphasize more on the accuracy improvement of a single predictor, and less on the stage identification and pattern merging of economic series in the front end of forecasting. Macroeconomic data often contain multiple operating states such as expansion, adjustment, shock and repair, and the correlation structure, amplitude characteristics and change rate of indicators are not consistent at different stages. If all the samples are directly sent to the unified prediction framework, the local fluctuation characteristics are easy to be averaged, and the structural differences within the series are difficult to fully enter the calculation process. Time series clustering analysis can group the change trajectories of multivariate economic series from the perspective of similarity measurement, compress the same kind of evolution patterns into computable state clusters, and then use the clustering results to guide the subsequent prediction structure to complete the targeted learning. This processing method takes into account data noise reduction, state division and pattern refinement, which not only enhances the clarity of input representation, but also improves the ability of the model to identify heterogeneous business cycles.

Based on this understanding, this paper constructs a time series clustering driven computing framework around macroeconomic forecasting tasks. The framework takes the multi-index sequence as input, extracts the stage pattern through the feature representation and clustering division module, and then empathizes the clustering results into the time series prediction structure to complete the joint estimation of the core economic variables and the comprehensive trend. After predicting the output, the residual correction unit continues to recalculate the deviation, so that the model can maintain the convergence characteristics and trend tracking ability during the rolling update process. The whole process follows the calculation link of "sequence representation - clustering division - time series prediction - residual correction - joint output", which emphasizes the coding, transmission and update of multi-source indicators. Compared with the prediction method of single-layer regression or single-path network, this design is more suitable for dealing with the phenomenon of long dependence and cross-variable coupling in macroscopic data.

The research objectives of this paper focus on three aspects: constructing a time series feature representation and clustering partition mechanism suitable for macroeconomic scenarios, so that the indicator evolution state enters the forecasting process in a structured way. A clustering-driven time series prediction structure was designed to make the model form a targeted calculation path after receiving the stage information, and enhance the ability to describe the multivariate association. The prediction residual correction and joint output mechanism are established to control the rolling error while maintaining the trend fitting ability of the model, and improve the stability and consistency under the time window.

2 Related work

Macroeconomic forecasting has gradually shifted from single indicator regression to multi-source data-driven computational modeling. Kapetanios and Papailias studied the role

of rapid indicators in economic evaluation, and proposed the processing idea of using high-frequency proxy variables to compress the time difference of statistical release, so as to make real-time judgment closer to the economic operation state [6]. Zheng et al. studied the joint modeling method of text information and macro indicators, and proposed to input semantic features and numerical sequences into the real-time prediction framework together to enhance the recognition ability of short-term business fluctuations [7]. Anesti et al. studied the prediction performance of machine learning methods on multiple sets of large-scale data, and proposed a cross-dataset parallel training and comparison strategy, indicating that multi-source input has a stable support effect on macroscopic prediction accuracy [8]. Silva et al. studied the role of international trade network in economic forecasting, and proposed to introduce network structure features into machine learning models to improve the computational expression of external conduction effects [9]. Bolivar studied the real-time GDP prediction method combining remote sensing data and machine learning, and proposed the technical path of non-traditional observation data participating in macro estimation, which expanded the data boundary of macro prediction [10]. Shams et al. studied GDP prediction in urban portrait scenarios and proposed a PC-LSTM-RNN combination structure, which combined dimensionality reduction processing and recurrent network into continuous prediction tasks [11].

The prediction of inflation and growth indicators has further promoted the application of deep learning methods in macro analysis. Stoneman and Duca studied deep learning methods in US inflation forecasting and proposed that machine learning can still maintain strong fitting ability in complex disturbance periods [12]. Naghi et al. studied the benefits of machine learning for inflation prediction and proposed new evidence to show that nonlinear models have advantages in indicator screening and forward estimation [13]. Das studied the analysis method of inflation rate prediction and its influencing factors, and proposed the calculation process of simultaneous processing of prediction and explanatory variable identification with machine learning framework [14]. Mirza et al. studied inflation forecasting in emerging economies and proposed to incorporate external variables such as foreign exchange reserves into the learning framework to improve forecasting performance in cross-market environments [15]. Adewale et al. studied the scheme of integrated machine learning for GDP prediction, and proposed that multi-model collaborative output can reduce the dependence of a single algorithm on local samples [16]. These studies show that macroeconomic forecasting has formed a technical route supported by high-frequency data, heterogeneous features and deep networks, but there is still room for continued refinement of the explicit division of intra-sample stage differences. From the perspective of implementation, these studies generally rely on feature engineering, sequence coding, parallel training, and error evaluation modules to operate in coordination, indicating that macroeconomic forecasting has become a typical computer data modeling task, and the model structure design and input organization jointly determine the quality of the results.

In order to more clearly present the differences in data sources, calculation methods and prediction tasks of existing studies, Table 1 summarizes the research contents, technical methods and main characteristics of the above representative literatures.

Table 1: Summary of related work

Author	Research Content	Technical Method	Main Feature
Kapetanios et al. [6]	Rapid Economic Assessment Using High-Frequency Indicators	High-Frequency Proxy Variables	Strengthens Real-Time Judgment
Zheng et al. [7]	Joint Forecasting with Text and Macroeconomic Data	Semantic Feature Fusion	Enhances Short-Term Identification
Anesti et al. [8]	Machine Learning Forecasting Across Multiple Datasets	Parallel Training and Comparison	Improves Multi-Source Adaptation
Silva et al. [9]	Economic Forecasting Based on Trade Networks	Network Feature Learning	Captures External Transmission Effects
Bolivar [10]	Remote Sensing-Driven GDP Forecasting	Remote Sensing and Machine Learning	Expands Data Sources
Shams et al. [11]	GDP Forecasting in Urban Scenarios	PC-LSTM-RNN	Strengthens Sequential Modeling

Research around time series clustering provides a more direct computational tool for macroeconomic phase identification. Lopez-Oriona et al. studied quantile fuzzy clustering of multivariate time series in frequency domain, and proposed a grouping mechanism to identify sequence similarity in frequency space [17]. Ghorbanian and Razavi studied the ensemble time series clustering method and proposed a fast clustering process for both speed and accuracy [18]. Li et al. studied the time series clustering method based on relationship network and community detection, and proposed a new path to construct clustering results by using structural links between sequences [19]. Benevento et al. studied the tail dependence clustering method with spatial constraints, and proposed to identify sequence clusters under the combined effect of correlation structure and spatial constraints [20]. Jorge and Ruben studied the random convolution kernel time series clustering method and proposed a clustering method that can extract local patterns without complex presets [21]. Existing results have shown that clustering methods can compress mode differences, enhance state representation and improve the quality of subsequent predictor input in high-dimensional time series data.

Based on the existing research, it can be seen that the computational framework of macroeconomic forecasting is shifting from single statistical estimation to multi-source data fusion and deep time series learning, and the clustering research has also extended from distance measurement to frequency domain, network and convolution representation. In contrast, research on macroeconomic scenarios still rarely uses time series clustering as the core part of the prediction front-end to organize the overall calculation process. Based on this understanding, this paper puts the macroeconomic time series feature representation, clustering division, time series prediction and residual correction into a unified framework, so that the clustering results are directly involved in the forecast structure driving and joint output calculation, so as to form a more suitable data analysis and forecast path for complex economic fluctuation environment.

3 Construction of macroeconomic forecasting model based on time series clustering analysis

3.1 Macroeconomic time series feature representation and clustering division

The front-end calculation of macroeconomic forecasting does not simply feed indicators such as growth, prices, employment, investment and foreign trade directly into subsequent forecasting structures. Different indexes have obvious differences in release time, statistical scale, fluctuation amplitude and response speed. The original series is also mixed with short-term disturbance, stage jump and local change. In order to make the subsequent prediction structure receive clearer and more stable state input, this section first completes the time series feature representation, and then implements the clustering partition within the unified representation space. After this process, the original discrete and scattered multivariate macro data will be reorganized into state clusters with stage characteristics, and the clustering results are then used as the conditional input of the subsequent time series prediction structure.

In order to clearly show the complete calculation link of the macroeconomic series from the original index input to the state cluster output, and illustrate the connection relationship between time window construction, frequency domain coding, fusion representation and cluster update, Fig. 1 shows the process structure adopted in the feature representation and cluster division stage in this paper. From left to right, the figure shows the transfer process of the original macroeconomic indicators after data preparation, time window construction, dual-channel coding in time domain and frequency domain, fusion representation generation and clustering module calculation. Finally, different macroeconomic state clusters such as expansion, recovery, slowdown and recession are formed, and stable stage label inputs are provided for subsequent prediction analysis.

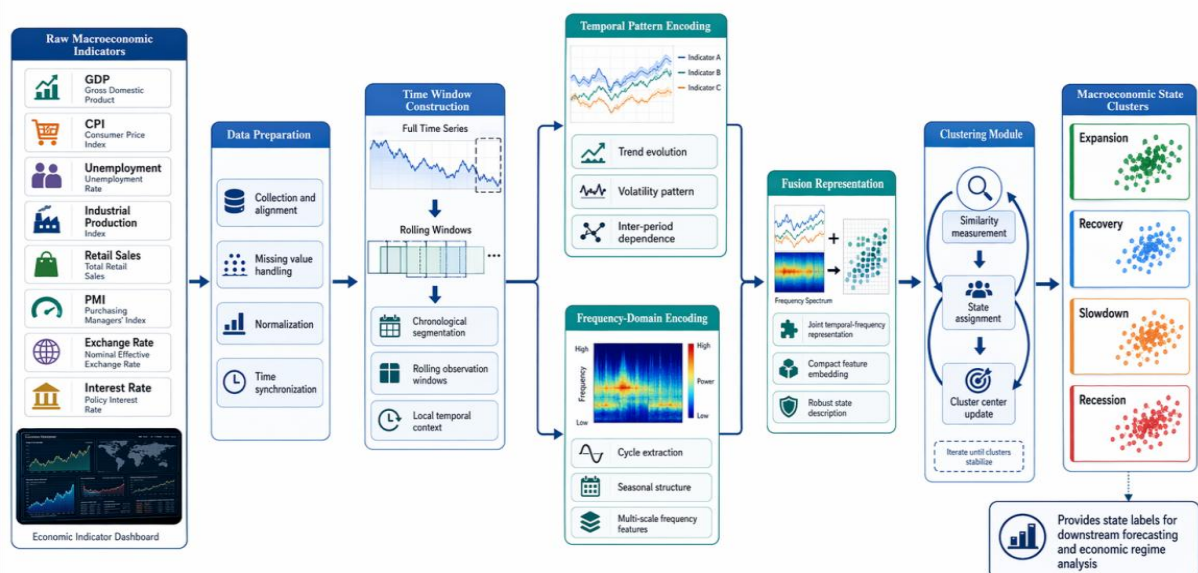


Figure 1: Flow chart of feature representation and clustering partition for macroeconomic time series

In order to make the macroeconomic indicators of different dimensions enter the unified calculation space and weaken the interference of extreme values on the subsequent clustering results while preserving the differences in the strength of fluctuations, this section first implements the robust standardization processing on the original series, as shown in Formula (1).

$$z_{i,t} = \frac{x_{i,t} - \text{Med}(x_i)}{\text{MAD}(x_i) + \varepsilon} \quad (1)$$

where $x_{i,t}$ denotes the original observed value of the i macroeconomic indicator at time t ; $\text{Med}(x_i)$ is the median of the index. $\text{MAD}(x_i)$ is the median absolute deviation. Let ε denote the stable term; $z_{i,t}$ denote the normalized eigenvalues. Formula (1) does not rely on the mean and variance, but adopts a more robust scale mapping method, so that sudden fluctuations will not be overly amplified, and lays a more stable numerical foundation for subsequent window construction and distance calculation.

After the scale mapping is completed, the discrete observations need to be organized into time window units with context relations, so that the local state, lag dependence and phase continuity can be preserved at the same time, and a unified sequence expression process can be entered, as shown in Formula (2).

$$h_t = [z_{t-w+1} \parallel z_{t-w+2} \parallel \cdots \parallel z_t] \quad (2)$$

Here, h_t denotes the window representation constructed with time t as the right endpoint. w is the window length. Let z_t denote the multi-index normalized vector at time t . \parallel denotes the vector concatenation operation. Formula (2) expands the original single-point macro observation into continuous time segments, so that the trend change and lag influence can be saved in the same window at the same time, so as to improve the integrity of subsequent feature coding.

It is still difficult to completely describe the periodic fluctuations, rhythm switching and local oscillations in macroeconomic variables only by relying on the time domain window. Therefore, this paper continues to extract the frequency domain response inside the window and jointly map it with the time domain representation to the fusion space. The specific calculation is shown in Formula (3).

$$r_t = [|\mathcal{F}(h_t)| \parallel \angle \mathcal{F}(h_t)] \quad (3)$$

Here, r_t represents the frequency domain response feature of window t ; $\mathcal{F}(\cdot)$ represents the discrete Fourier transform; $|\cdot|$ denotes the amplitude spectrum; $\angle(\cdot)$ represents the phase spectrum. Formula (3) extracts the change rhythm in the time window explicitly, so that the subsequent clustering division can identify the internal differences of different economic stages according to not only the value level, but also the fluctuation frequency and phase structure.

Considering the different contributions of different macro indicators in the switching of economic states, the simple concatenation of time domain and frequency domain features is still not enough to form a discriminative state representation. Therefore, this paper introduces the time attention weight in the fusion stage, and the specific calculation form is shown in Formula (4).

$$\mathbf{g}_t = \sum_{\tau=t-w+1}^t \alpha_{\tau,t} \mathbf{W}_h \mathbf{h}_\tau + \mathbf{W}_r \mathbf{r}_t + \mathbf{b}, \quad \alpha_{\tau,t} = \frac{\exp(\mathbf{q}_t^\top \mathbf{k}_\tau / \sqrt{d})}{\sum_{j=t-w+1}^t \exp(\mathbf{q}_t^\top \mathbf{k}_j / \sqrt{d})} \quad (4)$$

where \mathbf{g}_t represents the fused state vector; Let $\alpha_{\tau,t}$ denote the time weight; \mathbf{W}_h and \mathbf{W}_r denote the mapping matrix. \mathbf{b} represents the bias term; \mathbf{q}_t and \mathbf{k}_τ represent the query vector and key vector, respectively. d denotes the embedding dimension. Formula (4) strengthens the influence of key time points on the current state through weight allocation, so that signals such as growth, price and employment form a more hierarchical structure expression in the same representation vector.

In the state division stage, it is difficult to take into account amplitude difference, shape similarity and direction consistency at the same time by simply using Euclidean distance. Therefore, this paper uses a weighted measurement method composed of amplitude distance and correlation structure, and the specific calculation form is shown in Formula (5).

$$d(\mathbf{u}, \mathbf{v}) = \beta \|\mathbf{g}_u - \mathbf{g}_v\|_2 + (1 - \beta) \left(1 - \frac{\mathbf{g}_u^\top \mathbf{g}_v}{\|\mathbf{g}_u\|_2 \|\mathbf{g}_v\|_2} \right) \quad (5)$$

where $d(\mathbf{u}, \mathbf{v})$ is the comprehensive distance between sample \mathbf{u} and sample \mathbf{v} . β is the balance coefficient; $\|\cdot\|_2$ denotes the two-norm. Formula (5) incorporates numerical difference and structural similarity into the measurement at the same time, so that the clustering results are not only divided according to the degree of similarity in amplitude, but also can identify economic states with similar fluctuation patterns but different amplitudes, so as to improve the explanatory power of state clusters.

In order to make the clustering results have the three properties of compactness within a cluster, time continuity and separation between clusters at the same time, this paper constructs an optimization objective with timing constraints in the link of center updating and sample allocation, and its overall expression is shown in Formula (6).

$$J = \sum_{k=1}^K \sum_{t \in C_k} \omega_t \|\mathbf{g}_t - \mathbf{c}_k\|_2^2 + \lambda \sum_{t=2}^T \|\mathbf{g}_t - \mathbf{g}_{t-1}\|_2^2 - \gamma \sum_{1 \leq p < q \leq K} \|\mathbf{c}_p - \mathbf{c}_q\|_2^2 \quad (6)$$

where J represents the clustering optimization objective; K represents the number of state clusters; C_k represents the set of samples in the k cluster. Let ω_t denote the time weight; \mathbf{c}_k denotes the cluster center. Let λ denote the time continuity constraint coefficient; Let γ denote the inter-cluster separation coefficient. Equation (6) simultaneously incorporates the intra-cluster dispersion, sequence continuity and inter-cluster separation into the same objective function, so that the state division can not only maintain local convergence, but also reflect the true boundary between macroeconomic stages.

After the above processing, the original macroeconomic indicators are transformed into state clusters with stage attributes, and the clustering division results are then entered into the subsequent time series prediction structure. After feature screening, time-frequency domain fusion and state merging, the information sequence received by the prediction module is no longer the original sequence, but the conditional constraint information sequence, which makes the prediction result have a more explicit stage representation and enhances the stability of the calculation process.

3.2 Cluster-driven structure design for macroeconomic time series forecasting

After completing the feature representation and clustering division of macroeconomic time series, the input received by the forecasting end is no longer the unsorted original index set, but the state samples with stage attributes, fluctuation rhythm and local dependence information. In order to make the clustering results really participate in time series propagation and result generation, this section introduces six links into the prediction backbone: cluster center condition embedding, local time series extraction, clustering response calculation, state recursion, cross-variable relationship propagation and joint output decoding, so that the prediction structure can automatically adjust the internal calculation path according to the current stage. The prediction link formed in this way is no longer a time recursion on a single path, but integrates the recognition results of macroeconomic states, continuous time series characteristics and the linkage relationship between variables into the prediction process at the same time, so that different operating situations such as economic expansion, adjustment, shock and repair can obtain differentiated responses at the structural level.

In order to make the observation sample at the current time and the state center output by the clustering stage complete a unified expression at the input end, and introduce the time and position information into the prediction backbone together, this paper constructs the input fusion mapping for clustering conditions, and the specific form is shown in Formula (7).

$$e_t = \varphi(\Theta_x x_t + \Theta_c c_{k_t} + \Theta_p p_t + b_e) \quad (7)$$

where x_t represents the macroeconomic observation vector at time t , c_{k_t} represents the center vector of the cluster to which the current sample belongs, p_t represents the time position encoding, Θ_x , Θ_c and Θ_p represent the mapping parameters, b_e represents the bias vector, $\varphi(\cdot)$ represents the nonlinear mapping function, e_t represents the fused input representation. The function of this formula is to compress the numerical observation, stage state and time position information into the same computational space, so that the subsequent propagation unit has the stage awareness ability at the beginning, rather than waiting for the middle and late period to add external conditions.

In order to clearly show how the clustering results enter the backbone of time series forecasting and illustrate the connection relationship between input fusion, local extraction, state response and joint output, Fig. 2 shows the cluster-driven macroeconomic time series forecasting structure constructed in this paper. From left to right, the joint input process of current macroeconomic observation, clustering center information and time location information is presented. After conditional embedding, local time series extraction, clustering response weighting, state recursion and cross-variable relationship propagation, the multi-step macroeconomic forecasting results are finally output at the joint decoder.

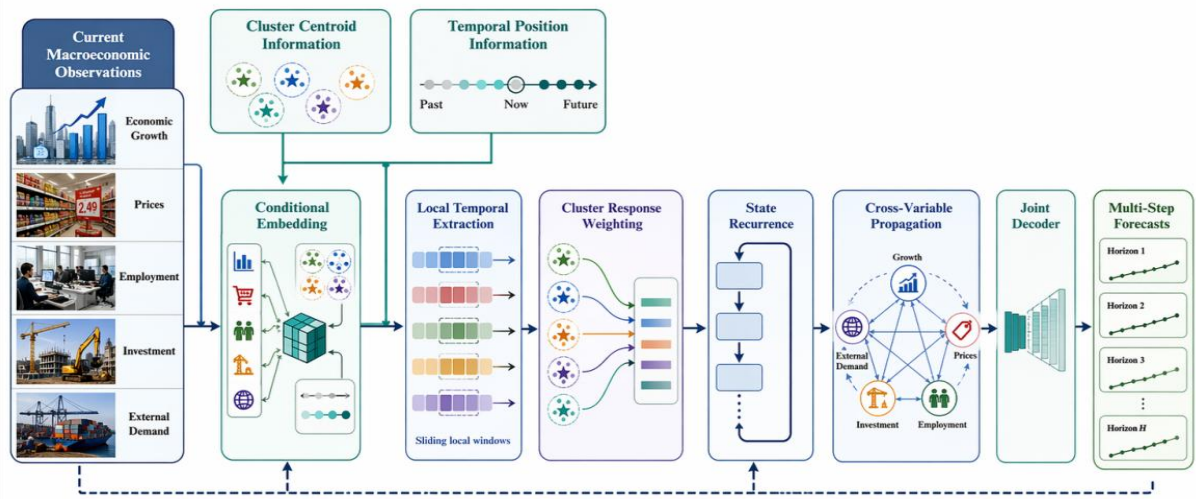


Figure 2: Graph of the structure of cluster-driven macroeconomic time series forecasting

In order to avoid the prediction structure only relying on a single point input and weakening the continuous change information in adjacent periods, this paper introduces a local time series extraction module after the fusion representation, which is used to depict the dynamic evolution characteristics within a short window. The specific form is shown in Formula (8).

$$q_t = \sum_{l=0}^{L-1} \Gamma_l e_{t-l} \quad (8)$$

Here, q_t represents the local temporal response vector at time t , L represents the decimation window length, Γ_l represents the temporal convolution parameter at the l position, and e_{t-l} represents the fusion input at the preceding time. This formula is not a simple sum, but a linear combination of each time in the window to extract short-term fluctuations, local inflection points and synchronous changes of adjacent indicators in advance, so as to provide more concentrated dynamic characteristics for subsequent state recurrence.

In order to make the prediction backbone not mechanically limited by a single cluster label, but able to form soft responses to multiple economic states according to the current input, this paper further constructs the cluster response weight calculation mechanism, the specific form is shown in Equation (9).

$$\alpha_{t,j} = \frac{\exp(q_t^T \Omega c_j)}{\sum_{r=1}^K \exp(q_t^T \Omega c_r)} \quad (9)$$

Here, $\alpha_{t,j}$ represents the response weight at time t to the j cluster center, Ω represents the matching matrix, c_j represents the j cluster center, and K represents the number of clusters. Formula (9) describes the closeness between the current time series state and the center of each stage. The greater the weight, the closer the current sample is to the corresponding economic stage. After processing in this way, the prediction structure no longer accepts only discrete classification results, but is able to perceive fuzzy boundaries in the stage transition interval in a continuous weight manner.

In order to make local dynamic information, historical state information and clustering stage information play a role together in the same propagation equation, this paper constructs the recursive expression of the state with clustering weighting term, and the specific form is shown in equation (10).

$$z_t = \tanh \left(\Lambda_q q_t + \Lambda_z z_{t-1} + \Lambda_a \sum_{j=1}^K \alpha_{t,j} c_j + b_z \right) \quad (10)$$

Here, z_t represents the hidden state at the current time, z_{t-1} represents the hidden state at the previous time, Λ_q , Λ_z and Λ_a represent the state transformation parameters, and b_z represents the bias vector. The key of this formula is to integrate the "current local temporal feature", "preorder memory state" and "cluster weighting center" into the same recursive process, so that the hidden state can not only maintain historical continuity, but also automatically correct the update direction according to the current stage.

In order to make the synchronous transmission relationship between indicators such as growth, price, employment and investment explicitly enter the prediction structure, rather than only implicitly absorbed by the recursive state, this paper further constructs the cross-variable relationship propagation mechanism after the hidden state, and the specific form is shown in Equation (11).

$$A_t = \text{softmax} \left(\frac{Q_t K_t^T}{\sqrt{d}} \right), \quad g_t = A_t V_t \quad (11)$$

Here, A_t represents the cross-variable relation matrix at time t ; Q_t , K_t and V_t represent the query, key and value matrices obtained from the current state mapping, respectively; d represents the scaled dimension; and g_t represents the state vector after relation propagation. Equation (11) is used to explicitly calculate the correlation response strength between each macro variable, so that the model can identify which indicators have stronger linkage effect at the current moment, thus providing structured relationship information for the output.

In order to make the final output retain the time recurrence results, relationship propagation results and clustering stage results at the same time, this paper constructs a joint decoding expression at the output side, and maps the multi-source states into the future multi-step macroeconomic forecast values in a unified manner, as shown in Formula (12).

$$\hat{y}_{t+\tau} = \Psi \left[z_t \parallel g_t \parallel \sum_{j=1}^K \alpha_{t,j} c_j \right] + b_o, \quad \tau = 1, 2, \dots, H \quad (12)$$

Here, $\hat{y}_{t+\tau}$ represents the prediction result at the τ future step, Ψ represents the output mapping matrix, b_o represents the output bias vector, \parallel represents the vector concatenation operation, and H represents the prediction step size. This formula decodes three types of information at the output, such as timing state, cross-variable relationship and stage center, so that the result given by the model is not only the general time inference value, but also the joint prediction result with stage conditions and relationship structure constraints.

After the above design, the clustering results have been transformed from the front-end grouping tool to the core condition information in the prediction backbone. The input fusion layer gives a phase-sensitive unified representation, the local extraction layer retains

short-term dynamics, the clustering response layer provides stage weights, the state recurrence layer realizes continuous propagation, the relationship propagation layer complements cross-variable linkage, and the joint output layer completes the final decoding. The time series prediction structure constructed in this way can provide a stable intermediate state and a clearer stage basis for the prediction residual correction and joint output mechanism in the next section.

3.3 Prediction residual correction and joint output mechanism

After the completion of the basic forecast, the backbone structure has been able to give multi-step macroeconomic output, but there will still be stage drift, local offset and error accumulation in the rolling extrapolation. In order to make the output have the ability of self-correction, this paper introduces the residual correction and joint output mechanism after the prediction backbone. The mechanism connected the basic prediction value, true feedback, hidden state and relationship state into the back-end link together. Through five steps of residual extraction, state coding, weight determination, result correction and joint optimization, the system deviation was continuously compressed and the consistency of cross-stage prediction was maintained.

To illustrate the connection order between the base prediction value, the true observation, the residual state, the correction weight and the final output, Fig. 3 shows the overall flow of the prediction residual correction and joint output mechanism. Then, the continuous deviation information is extracted by the state coding unit. Finally, the correction strength is determined according to the backbone state and the relationship state, and the corrected joint result is obtained.

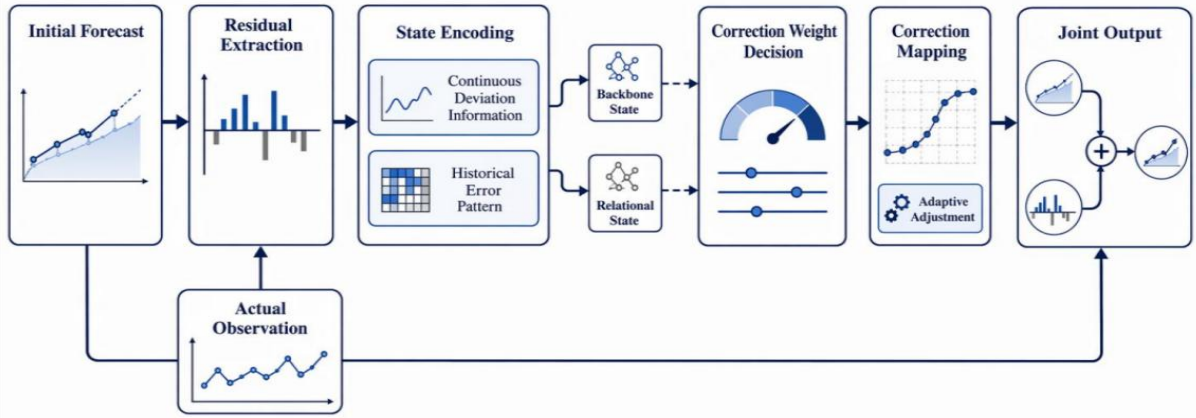


Figure 3: Flowchart of prediction residual correction and joint output mechanism

In order to transform the deviation information between the basic prediction results and the real observation into the calculation variables that can be continued propagated by the subsequent correction module, this section first defines the extraction form of the single-step residual, as shown in Formula (13).

$$r_t = y_t - \hat{y}_t \quad (13)$$

Here, y_t represents the true macroeconomic observation at time t , \hat{y}_t represents the base forecast, and r_t represents the single-step residual. The function of formula (13) is not limited to calculate the error size, but to explicitly transform the difference between the true feedback and the predicted output into a sequence variable that can be continued to

propagate, so that the correction module can dynamically update around the residual itself rather than around the static loss value.

In order to make the discrete residual form a continuous deviation representation, and compress the current error, preorder memory and predicted change rate into a single state space, this section constructs the residual state encoding equation, as shown in Formula (14).

$$\xi_t = \tanh(W_r r_t + U_r \xi_{t-1} + V_r \Delta \hat{y}_t + b_r) \quad (14)$$

Here, ξ_t represents the residual state vector at time t , ξ_{t-1} represents the residual state at the previous time, $\Delta \hat{y}_t$ represents the difference between the base predicted values of two adjacent steps, and W_r , U_r , V_r , and b_r represent the mapping parameters. Formula (14) incorporates the current error, historical error memory and predicted change rate into the same state update process at the same time, so that the residual coding result not only reflects the error amplitude, but also reflects the continuous direction and fluctuation trend of the error in the time dimension.

In order to enable the model to automatically adjust the error compensation proportion according to the current economic stage and the strength of cross-variable linkage, instead of imposing a fixed correction amplitude, this section further defines the correction weight, as shown in Formula (15).

$$\beta_t = \sigma(w_\beta^\top [\xi_t \| z_t \| g_t] + b_\beta) \quad (15)$$

where β_t represents the correction weight at time t , $\sigma(\cdot)$ represents the activation function, w_β and b_β represent the weight parameters and bias term, z_t represents the hidden state obtained by backbone time series propagation, g_t represents the state of cross-variable relationship propagation. Equation (15) is used to evaluate the sensitivity of the current sample to the residual correction, so that more targeted error compensation can be obtained in the high fluctuation stage and the structure switching stage.

In order to really project the residual state into the prediction space and complete the result correction without destroying the original trend expression, the gated correction equation is constructed in this section, as shown in Formula (16).

$$\tilde{y}_t = \hat{y}_t + \beta_t M \xi_t \quad (16)$$

Here, \tilde{y}_t represents the corrected output result, M represents the residual mapping matrix, and $\beta_t M \xi_t$ represents the dynamic correction term. Instead of simply stacking error values, Formula (16) controls the residual injection direction through weight adjustment and mapping transformation, so that the corrected results maintain the original trend structure while reducing local offset, thereby enhancing the stationarity and interpretability of the final output.

In order to make the base prediction accuracy, the corrected error and the smooth output simultaneously subject to a unified constraint in the training phase, this section further constructs the joint objective function, which is specifically shown in Equation (17).

$$L = \lambda_1 \|y_t - \hat{y}_t\|_2^2 + \lambda_2 \|y_t - \tilde{y}_t\|_2^2 + \lambda_3 \|\tilde{y}_t - \tilde{y}_{t-1}\|_2^2 \quad (17)$$

Here, L represents the joint training loss, λ_1 to λ_3 represent the weight coefficients of different objective terms, the first term measures the base prediction error, the second term measures the corrected output error, and the third term configures the smoothness of the

corrected output at adjacent moments. Equation (17) puts the three requirements of prediction, correction and stability into the same optimization framework, so that the model can form a consistent output convergence direction in the training stage.

In order to illustrate the responsibility allocation relationship of the above mechanisms in the overall link, Table 2 summarizes the input content, calculation goal and output results of the key modules in this section.

Table 2: Residual correction and description of the joint output module

Module	Input Content	Computational Objective	Output Result
Residual Extraction Layer	Ground Truth, Base Prediction	Generate the Error Sequence	r_t
State Encoding Layer	Residual, Historical State, Prediction Variation Rate	Compress Continuous Deviations	ξ_t
Weight Determination Layer	ξ_t, z_t, g_t	Estimate the Compensation Intensity	β_t
Output Correction Layer	Prediction, Correction Term	Complete Result Convergence	y_t

As can be seen from Table 2, this section does not consider residual correction as an additional step after backbone prediction, but rather designs it as a component running in synergy with state propagation and output decoding. The residual extraction layer is responsible for converting the real feedback into sequence variables, the state encoding layer is responsible for retaining the error memory, the weight judgment layer is responsible for determining the compensation amplitude, and the output correction layer is responsible for converting the deviation information into an executable adjustment.

4 Analysis of macroeconomic forecasting results based on the constructed model

4.1 Dataset selection and processing

This study uses multi-source macroeconomic data to construct experimental samples, and the data mainly come from the Open database of the World Bank, the International Financial Statistical Database of the International Monetary Fund, the OECD statistical database, the FRED Macroeconomic Series database and the quarterly reports publicly released by some national statistical institutions. In order to ensure the coverage of the series and the linkage of indicators, the sample selects the quarterly observations of 12 years from the first quarter of 2012 to the fourth quarter of 2023, covering 18 core indicators, including real GDP growth rate, CPI, unemployment rate, industrial value added, social consumption, fixed asset investment, exports, interest rate, exchange rate and manufacturing sentiment index. Finally, 24 economies and 1152 groups of valid samples were formed. The original data collected after the first completion of missing items identification and outlier screening, and then the combination of linear interpolation and local median correction is used to complete the completion, and the strong fluctuation index is implemented by quantile truncation and seasonal adjustment. Cross-source alignment is subsequently done with uniform quarterly timestamps, and dimensional differences are eliminated by robust normalization. In order to adapt the time series clustering and subsequent prediction structure, the processed data is

further reorganized into fixed-length samples according to the sliding window, while retaining the stage label, the window position encoding and the real output value. The training set, validation set and test set were divided into 7:1.5:1.5, and all processing processes were completed in the Python environment, so as to ensure the consistency of model input, computability and reproducibility of results. In the modeling phase, the 18 indices are mapped into multivariate tensors, and the clustering input matrix, prediction input matrix and residual correction target sequence are generated synchronously. To avoid time leakage, the window segmentation strictly follows the order of observation first and prediction later, and all the normalization parameters are only calculated based on the training set statistics. For the indicators with different release frequencies, the study uses quarterly aggregation and the most recent alignment to complete the unified coding, and enhances the stability and accuracy performance of subsequent calculations.

4.2 Model comparison experiment

In order to test the actual performance of the constructed model in macroeconomic forecasting tasks, this paper compares TSC-MEP with ARIMA, SVR and single LSTM, and analyzes it from four aspects: error control, prediction accuracy, comprehensive recognition ability and threshold discrimination ability. Fig. 4 shows the error results of the four classes of models on the test set. It can be seen that TSC-MEP is at the lowest level in the three indicators of mean square error, mean absolute error and root mean square error, where mean square error is 1.67%, mean absolute error is 2.14%, and root mean square error is 2.36%. The corresponding results for single LSTM are 3.92%, 4.11% and 4.43%, 5.28%, 5.74% and 6.02% for SVR, and 6.13%, 6.58% and 6.91% for ARIMA. This result indicates that the adaptation ability of the model to local fluctuations, stage switching and multivariate coupling is significantly enhanced after the clustry-driven structure enters the prediction backbone, and the deviation between the predicted value and the true observation is compressed to a smaller range.

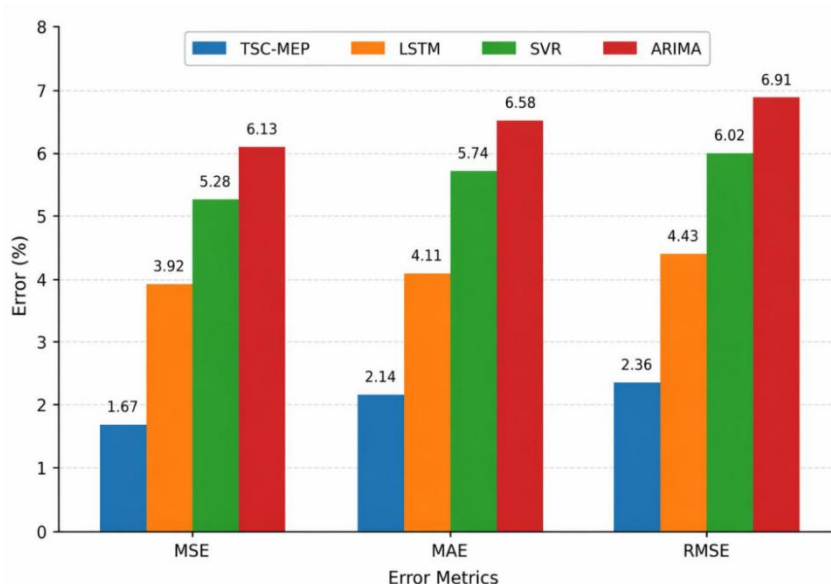


Figure 4: Comparison plots of error metrics for four types of models

The error difference in Fig. 4 does not only reflect the change of numerical value, but also reflects the ability of different models to capture the boundary of economic state transition. ARIMA can still maintain the basic fitting in the continuous stationary interval,

but the error will be significantly amplified when the sample segment with short-term contraction and rapid recovery coexists. SVR has a certain ability to maintain local mapping relationships, but it is difficult to stably undertake intertemporal dependencies in long sequences. Single LSTM can improve long-term memory representation, but it still lacks stage information constraints. After TSC-MEP embeds the time series clustering division results into the prediction backbone, the samples before and after the state switch are no longer mixed into the same calculation path, so the error decrease is more obvious.

To further compare the prediction consistency of different models on the test subset, Fig. 5 shows the accuracy results of the four classes of models in the five groups of test samples. The accuracy of TSC-MEP on the five groups of data reaches 92.84%, 93.76%, 94.11%, 92.95% and 93.39%, respectively, and the average value is 93.41%. The average accuracy of single LSTM is 86.27%, SVR is 81.54%, and ARIMA is 78.63%. It can be seen from the figure that TSC-MEP not only has the highest overall accuracy, but also has the smallest inter-group fluctuation, which indicates that the model maintains a relatively stable output structure in different economic intervals without obvious local distortion.

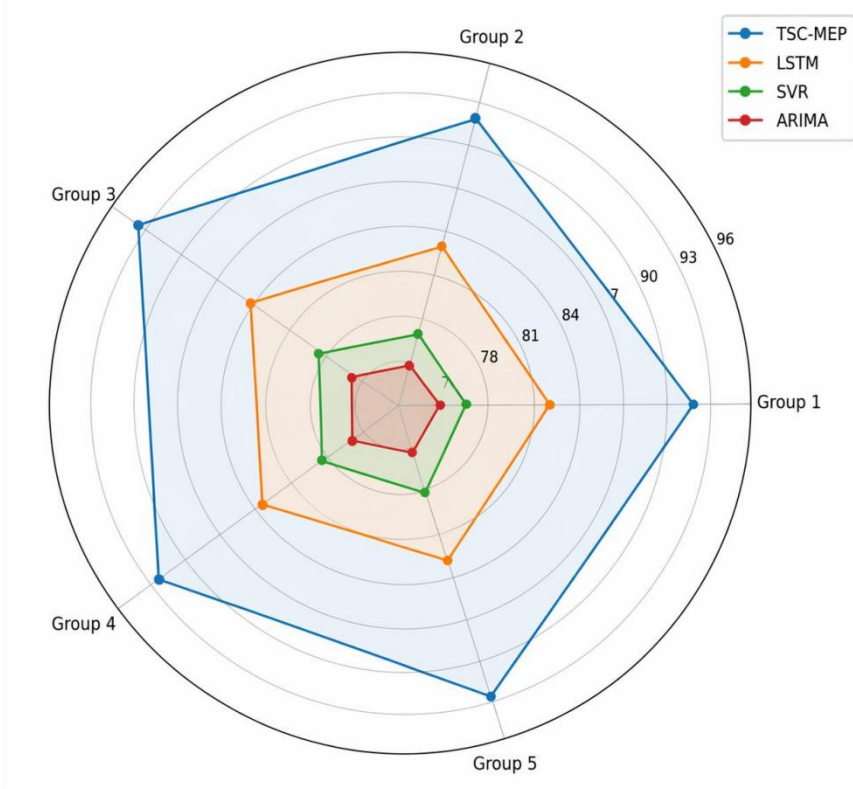


Figure 5: Radar plot of average prediction accuracy of four classes of models

The accuracy results show that the stage labels and state centers provided by the clustering front end are not additional information, but rather important conditions that determine the quality of the prediction. When the input sequence is in different stages such as expansion, repair or slowdown, TSC-MEP can automatically adjust the hidden representation and output map according to the state weight, so it maintains similar recognition ability for multiple sets of samples. Although single LSTM can track the basic trend, it is prone to offset in the local oscillation interval. SVR and ARIMA are more susceptible to the influence of sample structure differences, resulting in obvious fluctuations in the prediction results between different subsets.

In order to investigate the comprehensive performance of the models in the business state recognition task, Fig. 6 shows the F1 value distribution of the four types of models on the test set. The F1 value of TSC-MEP stably distributed between 0.89 and 0.93, and the average value was 0.912. The average value is 0.846 for single LSTM, 0.781 for SVR, and 0.742 for ARIMA. The higher and more concentrated F1 distribution indicates that TSC-MEP achieves a more stable balance between precision and recall, and has stronger recognition ability for samples near the boundary between expansion and contraction.

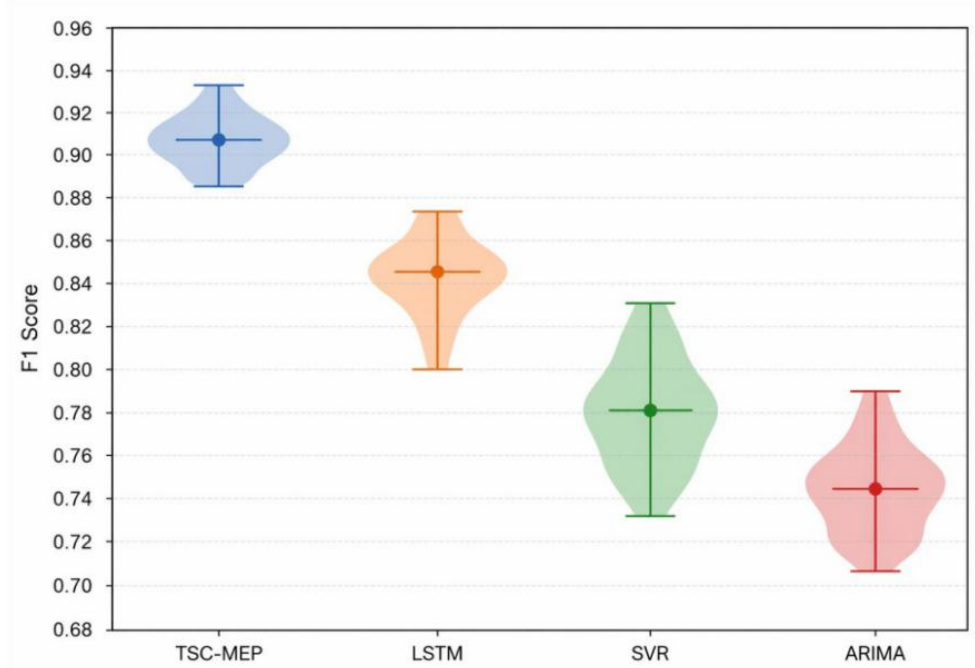


Figure 6: F1-value distribution plots for four classes of models

It can also be seen from Fig. 6 that the dispersion range of TSC-MEP is significantly smaller than that of the remaining three types of models, which means that the output changes of the model in multiple test Windows are more controllable. There are often complex signals such as weak growth, low inflation and investment decline in the macroeconomic sequence at the same time, and simply relying on a single path recurrence is easy to cause category judgment bias. When the cluster-driven structure and the relationship propagation module work together, the model can maintain smoother recognition results in complex combination states, thereby improving the stability of multi-index joint prediction.

In order to evaluate the discriminative ability of different models under threshold changes, Fig. 7 shows the ROC curve and AUC results of the four classes of models. The AUC of TSC-MEP is 0.931, single LSTM is 0.872, SVR is 0.816, and ARIMA is 0.791. The results show that TSC-MEP can maintain a high true positive rate and control the false positive rate in a low range under different decision thresholds, and the output results have better discrimination stability.

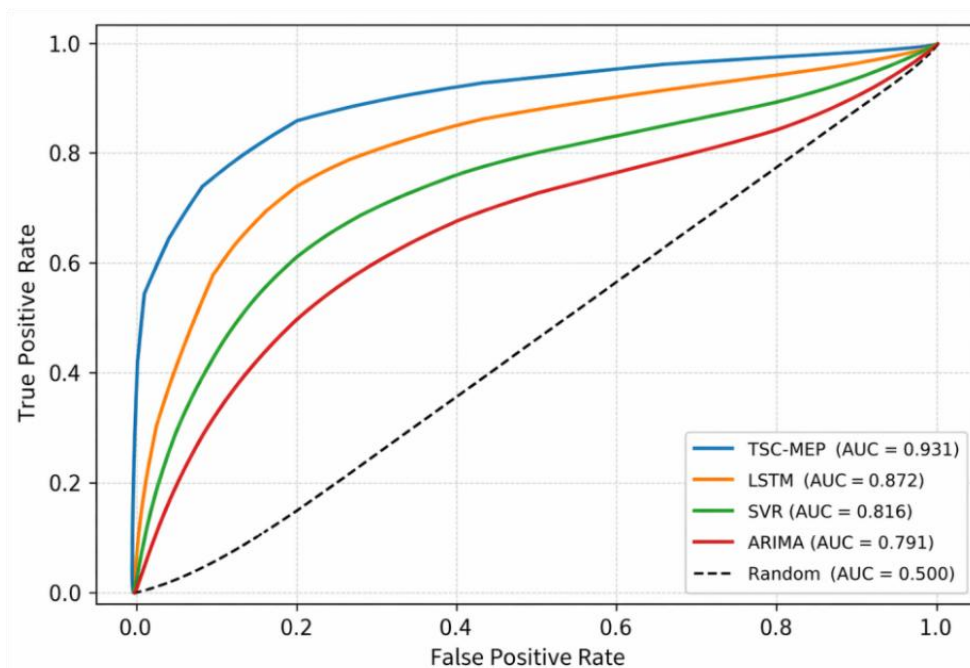


Figure 7: Comparison plot of ROC curves for four classes of models

Based on the above, it can be seen that TSC-MEP is superior to the comparison models in terms of error control, accuracy improvement, comprehensive recognition ability and threshold robustness. After the time series clustering analysis completes the stage division in the front end, the prediction backbone obtains a clearer state boundary. The cross-variable relationship propagation further enhances the expression of economic linkage. The residual correction module in turn compresses the local bias at the output. After the three parts work together, the model shows higher accuracy, more stable output and stronger application adaptation ability in macroeconomic forecasting tasks.

4.3 Application effect and stability test of macroeconomic forecasting

In order to test the applicability of the model in real macroeconomic analysis scenarios, this paper selects the data of 24 economies from the first quarter of 2019 to the fourth quarter of 2023 as the application verification interval, focusing on the joint forecasting performance of growth, price, employment, investment, external demand and interest rate under different economic stages.

To present the recognition distribution of the model for different economic states, Fig. 8 shows the heat maps of the four types of macro stages in the test interval. The horizontal is the quarterly series, the vertical is the 24 economies, and the color shades indicate the phase intensity of the model output. The results show that the contraction signal is most concentrated in the second quarter of 2020, the recovery state gradually spreads in the middle and late 2021, and a local slowdown occurs from late 2022 to mid-2023, while the expansion state is mainly concentrated in the post-2023 period. The hot spot distribution is basically consistent with the actual macro fluctuation rhythm, indicating that the model can project the multi-index changes into a stage picture with temporal and spatial readability.

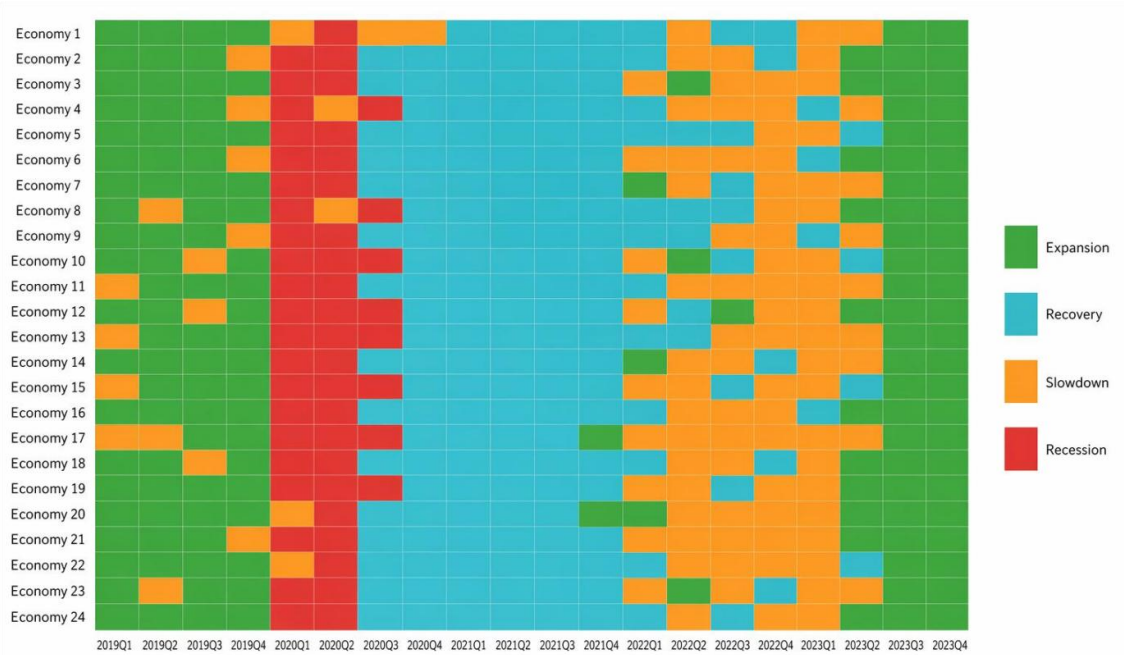


Figure 8: Heatmap of macroeconomic stage identification

To illustrate the prediction bias versus fitting level on different regional samples, Table 3 presents the application results for the four regional test groups. It can be seen that the mean absolute errors of TSC-MEP in North America, Europe, East Asia and emerging economies are 2.08%, 2.19%, 2.27% and 2.41%, respectively, and the corresponding goodness of fit reaches 0.931, 0.924, 0.918 and 0.906, respectively. The regional results show that the model performs more stably in economies with higher index completeness and also maintains better output continuity in the more volatile emerging sample.

Table 3: Comparison table of regional application results

Region	MAE / %	RMSE / %	R ²
North America	2.08	2.31	0.931
Europe	2.19	2.44	0.924
East Asia	2.27	2.53	0.918
Emerging Economies	2.41	2.68	0.906

To observe the degree of stability of the model in multi-step rolling forecasts, Table 4 lists the error changes under 1-step, 2-step, 4-step and 6-step forecasts. The results show that the error increases with the increase of the prediction step, but the increase slope is slow: MAE increases from 1.96% to 2.58%, and RMSE increases from 2.11% to 2.87%. This result shows that the cluster-driven structure and residual correction module can still maintain good error constraint ability in long step size prediction.

Table 4: Multi-step rolling prediction stability test table

Prediction Horizon	MAE / %	RMSE / %	AUC
1-Step	1.96	2.11	0.943
2-Step	2.07	2.26	0.938
4-Step	2.31	2.55	0.928
6-Step	2.58	2.87	0.914

To examine the contribution of each component module to the final performance, Table 5 further presents the ablation experiment results. After removing the clustering-driven module, the average accuracy decreased from 93.41% to 89.26%. After removing the relationship propagation module, it reduced to 90.14%. After removing the residual correction module, it was reduced to 90.83%. The full model remains optimal. Ablation results show that clustering division, cross-variable propagation and error correction are not simple superposition, but form a synergistic relationship within the prediction structure.

Table 5: Table of ablation experiment results

Model Setting	Accuracy / %	F1	AUC
Without Clustering-Driven Module	89.26	0.871	0.896
Without Relation Propagation	90.14	0.882	0.904
Without Residual Correction	90.83	0.889	0.911
Full Model	93.41	0.912	0.931

Taking the above into account, it can be seen that TSC-MEP can not only form clear stage identification results in real macroeconomic scenarios, but also maintain high stability in regional differences, long-step rolling forecasts and module pruning tests. The results show that the forecasting framework constructed in this paper can provide reliable computational support for macroeconomic monitoring, boom judgment and trend analysis.

5 Discussion

Compared with macroeconomic forecasting research, the time series cluster-driven framework constructed in this paper does not only use clustering as a pre-grouping tool, but directly embed state cluster information into the process of time series propagation, cross-variable relationship modeling and residual correction, so that the forecasting structure can adjust its internal response path around the change of economic stage. The experimental results are supported by data. The mean square error, mean absolute error and root mean square error of TSC-MEP on the test set are 1.67%, 2.14% and 2.36%, respectively, which are significantly lower than 3.92%, 4.11% and 4.43% of LSTM. The prediction accuracy of the five groups of test samples reaches 93.41%, which is higher than 86.27% of LSTM, 81.54% of SVR and 78.63% of ARIMA. The F1 value of the model is 0.912, and the AUC reaches 0.931. The test shows that the mean absolute errors of the framework in North America, Europe, East Asia and emerging economies are 2.08%, 2.19%, 2.27% and 2.41%, respectively, and the goodness of fit remains between 0.906 and 0.931. When the prediction step is increased from 1 to 6, MAE increases from 1.96% to 2.58%, and RMSE increases from 2.11% to 2.87%. These results show that the synergy of time series clustering analysis, relationship propagation and residual correction in the unified link can enhance the adaptation ability of the model to multivariate linkage, stage switching and long-step rolling prediction, and also make the method valuable in business tracking, cycle identification and regional comparison analysis. Further combined with the ablation experimental results, it can be seen that after the clustering-driven module is removed, the accuracy of the model decreases to 89.26%, the F1 value decreases to 0.871, and the AUC decreases to 0.896, indicating that the stage division is not a peripheral auxiliary design, but an important basis for determining whether the predicted path can maintain a clear boundary. After removing the relationship propagation module, the model's ability to capture the linkage relationship between growth, price, employment and investment is weakened, and the accuracy drops to

90.14%, which indicates that if the synchronous transmission between macro variables cannot enter a unified expression space, the prediction results are prone to local deviation. After removing the residual correction module, the accuracy is 90.83%, and the AUC is 0.911, which shows that the error recovery mechanism at the output has a direct impact on the stability of multi-step prediction. Based on the results of regional experiments, rolling prediction and module pruning, it can be judged that the advantages of the proposed model are not only reflected in the decline of a single error index, but also reflected in the stable results maintained under different economic stages, different regional samples and different prediction step sizes, which is the main performance that distinguishes it from traditional statistical models and single path depth models.

6 Conclusions

Focusing on the forecasting task of macroeconomic multi-indicator time series data, this paper constructs a computational framework that integrates time series clustering, stage response propagation and residual joint correction. Experimental results show that the proposed framework is superior to the comparison methods in terms of error control, stage identification and multi-step output stability, and can better adapt to complex scenarios where variables such as growth, price, employment and investment change together. At the same time, the research shows that the state boundary provided by the clustering front-end helps to improve the quality of input representation, the relationship propagation structure strengthens the cross-variable linkage expression, and the residual correction mechanism further compresses the local offset in rolling prediction. However, this paper still has some limitations. Although the sample covers multiple economies, the frequency of indicators is still quarterly data, and there is still room to compress the immediate response to higher frequency shocks. The number of clusters and window length depend on the selection of validation set, and there are still differences in the optimal structure between different economies. Model training has certain requirements on continuous data quality and computing power conditions, and the output stability is still affected in the extreme sparse sample environment. Follow-up research can continue to introduce monthly high-frequency indicators, text information and cross-market network data, build a finer-grained state division method, and further carry out lightweight deployment, adaptive parameter update and cross-regional transfer learning, so as to enhance the application ability of the model in real-time monitoring and intelligent decision-making scenarios. These directions will enable the model to achieve faster response speed, higher interpretability, and more stable deployment ability across scenarios while maintaining prediction accuracy. It will also provide more stable and continuous data support for economic analysis, risk identification and policy research.

References

- [1] Goulet Coulombe P, Leroux M, Stevanovic D, et al. How is machine learning useful for macroeconomic forecasting?[J]. *Journal of Applied Econometrics*, 2022, 37(5): 920-964.
- [2] Longo L, Riccaboni M, Rungi A. A neural network ensemble approach for GDP forecasting[J]. *Journal of Economic Dynamics and Control*, 2022, 134: 104278.
- [3] Lin S L. Application of empirical mode decomposition to improve deep learning for

- US GDP data forecasting[J]. *Heliyon*, 2022, 8(1).
- [4] Wang Y, Su C W, Zhang Y, et al. Effectiveness of Principal-Component-Based Mixed-Frequency Error Correction Model in Predicting Gross Domestic Product[J]. *Mathematics*, 2023, 11(19): 4144.
- [5] Zhang Q, Ni H, Xu H. Nowcasting Chinese GDP in a data-rich environment: Lessons from machine learning algorithms[J]. *Economic Modelling*, 2023, 122: 106204.
- [6] Kapetanios G, Papailias F. Assessing the economy using faster indicators[J]. *Journal of Forecasting*, 2024, 43(1): 208-223.
- [7] Zheng T, Fan X, Jin W, et al. Words or numbers? Macroeconomic nowcasting with textual and macroeconomic data[J]. *International Journal of Forecasting*, 2024, 40(2): 746-761.
- [8] Anesti N, Kalamara E, Kapetanios G. Forecasting with machine learning methods and multiple large datasets[J]. *Econometrics and Statistics*, 2024.
- [9] Silva T C, Wilhelm P V B, Amancio D R. Machine learning and economic forecasting: The role of international trade networks[J]. *Physica A: Statistical Mechanics and its Applications*, 2024, 649: 129977.
- [10] Bolivar O. GDP nowcasting: A machine learning and remote sensing data-based approach for Bolivia[J]. *Latin American Journal of Central Banking*, 2024, 5(3): 100126.
- [11] Shams M Y, Tarek Z, El-kenawy E S M, et al. Predicting Gross Domestic Product (GDP) using a PC-LSTM-RNN model in urban profiling areas[J]. *Computational Urban Science*, 2024, 4(1): 3.
- [12] Stoneman D, Duca J V. Using deep (machine) learning to forecast US inflation in the COVID-19 era[J]. *Journal of Forecasting*, 2024, 43(4): 894-902.
- [13] Naghi A A, O'Neill E, Danielova Zaharieva M. The benefits of forecasting inflation with machine learning: New evidence[J]. *Journal of Applied Econometrics*, 2024, 39(7): 1321-1331.
- [14] Das P K, Das P K. Forecasting and analyzing predictors of inflation rate: Using machine learning approach[J]. *Journal of Quantitative Economics*, 2024, 22(2): 493-517.
- [15] Mirza N, Rizvi S K A, Naqvi B, et al. Inflation prediction in emerging economies: Machine learning and FX reserves integration for enhanced forecasting[J]. *International Review of Financial Analysis*, 2024, 94: 103238.
- [16] Adewale M D, Ebem D U, Awodele O, et al. Predicting gross domestic product using the ensemble machine learning method[J]. *Systems and Soft Computing*, 2024, 6: 200132.
- [17] López-Oriona Á, Vilar J A, D'Urso P. Quantile-based fuzzy clustering of multivariate

- time series in the frequency domain[J]. *Fuzzy Sets and Systems*, 2022, 443: 115-154.
- [18] Ghorbanian A, Razavi H. A new method based on ensemble time series for fast and accurate clustering[J]. *Data Technologies and Applications*, 2023, 57(5): 756-779.
- [19] Li H, Du T, Wan X. Time series clustering based on relationship network and community detection[J]. *Expert Systems with Applications*, 2023, 216: 119481.
- [20] Benevento A, Durante F, Pappadà R. Tail-dependence clustering of time series with spatial constraints[J]. *Environmental and Ecological Statistics*, 2024, 31(3): 801-817.
- [21] Jorge M B, Rubén C. Time series clustering with random convolutional kernels: MB Jorge and C. Rubén[J]. *Data Mining and Knowledge Discovery*, 2024, 38(4): 1862-1888.